J. Phys.: Condens. Matter 5 (1993) 6971–6982. Printed in the UK

Bandstructure of two-dimensional periodic potentials in a magnetic field: a recursive Green-function approach

R B S Oakeshott and A MacKinnon
Blackett Laboratory, Imperial College, London SW7 2BZ, UK

Received 1 February 1993

Abstract. We show how the bulk band conductivity and density of states of an electron gas in a general two-dimensional periodic potential and magnetic field can be calculated using the recursive Green-function method. Computational efficiency is maximized by using the gauge symmetry of the problem. As an example we show the conductivity and density of states for a superlattice displaying the recursive Hofstader's-butterfly spectrum.

1. Introduction

The band structure of a two-dimensional electron gas 2DEG subject to a periodic potential and a magnetic field has an intricate structure depending on the number of flux quanta per unit cell of the periodic potential. In simple cases such as a weak potential [1–3], a tight-binding band [1, 4], hopping between edge states [5] the magnetic field produces a recursively split spectrum.

Experiments on lateral-surface superlattices [6–10] approach the point where effects due to the splitting of the spectrum may be apparent. Real experiments however are generally performed with many electrons in each unit cell, and so many overlapping bands; with inelastic scattering; with a random potential from impurities; potentially with the periodic potential and the cyclotron energy of similar magnitudes; and with the magnitude of hopping terms between states in different unit cells depending on the magnetic field and the Fermi energy. We focus in this paper on the bulk effects which are likely to show the effects of band gaps in a simpler form than situations where edges are important [5]. In practical experiments, the effects of edge states may or may not be important, depending on the geometry of the sample, and the measurement being made.

In this paper we show how the recursive Green-function method can be used to calculate the bulk band conductivity and density of states of lateral-surface superlattices. The paper is organized as follows. In section 2 we introduce the single-electron model used. We solve the model by approximating the continuous Hamiltonian by a discrete Hamiltonian on a square lattice, and we discuss the approximations and advantages involved in this in section 3. In section 4 we show how a minimal unit cell can be constructed, taking advantage of the gauge symmetry of the problem, and how the gauge symmetry can be used to calculate economically the Green function of a unit cell using the recursive Green-function technique. In section 5 we show how the conductivity of the infinite, periodic system can be found from the Green function of the isolated unit cell, by using a small imaginary component to the energy to probe the group velocities of the states. In section 6 we show how the density of states can be found from the derivatives of the wavenumber with respect to the energy. In section 7 we show as an example calculations of the Hofstader's butterfly [4] for this model.

0953-8984/93/376971+12$07.50

2. Model

We adopt the simplest model for the electrons at the interface of a GaAs/AlGaAs heterostructure, and use the single-particle Hamiltonian

$$H\psi = (1/2m^*)(p - eA)^2\psi + V\psi \tag{1}$$

for an electron confined to the x-y plane, subject to an effective potential V, with a perpendicular magnetic field, and with an effective mass m^*. In taking a single-particle picture, we are neglecting at the outset correlations, both of the Coulomb blockade [11–14] and of the fractional quantum Hall effect forms [15, 16].

Both the periodic and random parts of the potential V are self-consistent functions of the structure of the device, the applied gate voltage, and the distribution of ionized donors. We do not attempt to calculate the form of V but consider the effect of a reasonable, fixed periodic potential, and include the effects of the random potential in a scattering time. As the density of states of the system varies the scattering time will vary, both because the phase space available to scatter into will change [17, 18], and because the potential will vary as the screening length changes [19, 20]. We have not attempted to calculate the scattering time self-consistently, but instead assume a fixed scattering time.

With the assumptions of a fixed scattering time and periodic potential, we calculate the longitudinal conductivity from a simple kinetic equation[21]

$$\sigma_{xx} = \frac{e^2\tau}{A}\sum_{k_x}\sum_{k_y}\sum_{n} v_x^2\left(-\frac{\partial f}{\partial E}\right) \tag{2}$$

where τ is the transport scattering time, v_x is the group velocity of the mode in the x direction, A is the area of the system, and f is the Fermi–Dirac distribution function.

Equation (2) is valid so long as it is a reasonable approximation to assume that electrons are scattered to a random mode, without regard to the distribution of the wavefunction, and so long as one can characterize the motion of the electrons by their group velocity. The first assumption is inappropriate where the conductivity is dominated by (spatially separated) edge states as for the quantum Hall effect [16, 22–24]. The second assumption implies that the mean free path of a (Bloch) electron must be large compared to the lattice period. We therefore need $v_x\tau \gg a$. Using the Einstein relation, $\sigma = \rho(E_F)e^2D$, where D is the diffusion constant, and ρ is the density of states, we require

$$\sigma \gg \frac{\rho(E_F)e^2a^2}{\tau} \tag{3}$$

where a is the lattice period.

For the single-electron picture to be appropriate, we must be able to neglect electron–electron correlations due to the Coulomb interaction. A basic requirement is that the bandwidth be large compared with a typical Coulomb energy. The worst case is for low Fermi energies, where there is of the order of one electron per unit cell, and the Coulomb interaction at short distances will only be screened by remote electrons in the gates. The interaction energy will then be of the order of

$$E_Q \simeq e^2/4\pi\epsilon_0\epsilon_r a. \tag{4}$$

For a lattice periodicity of 100 nm, E_Q is approximately 1 meV. For higher Fermi energies, screening by electrons in the 2DEG will reduce the interaction energy.

3. Discrete Hamiltonian

We approximate the continuum Hamiltonian (1) by a discrete Hamiltonian on a square lattice [25] with on-site potential $H_{ii} = V(r_i)$ and nearest-neighbour hopping terms $H_{ij} = v_0 \exp(-i\phi)$ where

$$v_0 = \hbar^2/2m^*|\Delta r|^2 \tag{5}$$

and

$$\phi = eA \cdot \Delta r/\hbar. \tag{6}$$

where $\Delta r = r_j - r_i$. The phase ϕ ensures that the product round any loop of the hopping terms has a phase $2\pi\Phi/\Phi_0$, where Φ is the magnetic flux through the loop, and Φ_0 is the single electron flux quantum h/e. A is taken to be defined on the bonds of the lattice.

The use of a discrete real-space Hamiltonian, rather than using a Landau-level basis, has several advantages: it is easier to study arbitrary potentials, and in particular hard-wall-antidot, type potentials; the method can be applied easily to cases where the magnetic field is modulated and the Landau states do not diagonalize the Hamiltonian even in the absence of an electrostatic potential; it is easy to extract the real-space density of states; and it is an approach that can also be applied to finite systems, making it easier to see the effect of introducing edges into the system.

The use of a discrete Hamiltonian gives rise to errors for Fermi energies that are large compared with the bandwidth of the discrete lattice, we must therefore have $E_F \ll v_0$. We also expect significant errors for magnetic fields where the magnetic length is small relative to the period of the lattice, (or equivalently where the number of flux quanta per square of the discrete lattice is not much less than unity), so we need $B\Delta r^2 \ll h/e$. If the magnetic length is not large compared with the lattice spacing, then Landau levels, which should be dispersionless, acquire a dispersion determined by the difference in energy between a state centred on a lattice site, and a state centred between two lattice sites. A simple estimate of the magnitude of the effect can be found by taking the continuum wavefunction for the lowest Landau level, which, in the Landau gauge, is

$$\Psi(x, y) \propto \exp[-(x - x_0)^2/(2l_B^2)] \exp(iky), \tag{7}$$

and finding the expectation value of the energy of this wavefunction with the discrete Hamiltonian. The difference between the energy of the state centred on the a lattice site, and that between two lattice sites, is approximately proportional to

$$v_0 \exp[-4.3(l_b/\Delta r)^2] \tag{8}$$

for $l_b > \Delta r$. The dispersion is therefore essentially zero when l_b is significantly greater than the lattice spacing.

4. Unit cell in a magnetic field

Since the properties of a physical system are expected to vary continuously with the magnetic field [4], we restrict our calculation to magnetic fields with a rational number of flux quanta

per unit cell. By choosing a suitable gauge, we can then construct a unit cell that contains an integer number of superlattice cells, and of flux quanta.

Consider a magnetic field with p/q flux quanta to each unit cell of the super-lattice potential. We use the vector potential

$$\begin{aligned} A_x &= -B(y \bmod a)(qa/\Delta x)\{\mathrm{int}(x/qa) - \mathrm{int}[(x+\Delta x)/qa]\} \\ A_y &= -B(x \bmod qa) \end{aligned} \tag{9}$$

where the coordinates of the bonds are the coordinates of their lower left-hand ends, and Δx and Δy are the lengths of the bonds in the x and y directions. The combined vector and superlattice potential is then periodic in the x direction with period qa, and in the y direction with period a. This potential, which looks complicated, is essentially a conventional vector potential using the Landau gauge, $\boldsymbol{A} = (0, -Bx, 0)$, with a gauge transform $A_y \mapsto A_y - nBqa$ where n labels different unit cells in the x direction. The A_x terms ensure that

$$\nabla \times \boldsymbol{A} = \sum_{\text{loop}} \boldsymbol{A} \cdot \Delta \boldsymbol{r}/a^2 = B \tag{10}$$

for every cell of the discrete lattice. In a continuum Hamiltonian this gauge would be discontinuous, but there are no problems within the discrete representation.

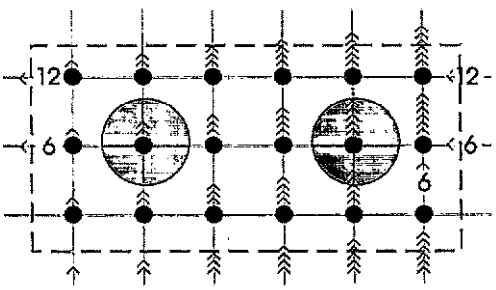

Figure 1. Vector potential for a magnetic field with half a flux quantum per unit cell and a 3 × 3 lattice for each unit cell of the superlattice potential. Each arrow represents a phase of $\exp(i\pi/18)$.

The vector potential used is more readily understood by an example. Figure 1 shows schematically the potential for a magnetic field with half a flux quantum to each period of the onsite superlattice potential. The size of the unit cell is chosen so that the phase on the bonds in the x direction between unit cells is periodic with the width of the unit cell.

4.1. Recursive Green-function method

Since we have to handle unit cells q times larger than the unit-cell size needed to represent the superlattice potential, we need a method which scales well to large system sizes. The recursive Green-function method is one such [26–29].

The method is now standard (see Sols *et al* [29] for details) and we simply remind the reader of the bare outline. The Green function of a small part of the system is found analytically, or by solving the matrix equation $(\mathbf{E} - \mathbf{H})\mathbf{G} = \mathbf{I}$ for the small system. The system is enlarged by successively solving Dyson's equation, $\mathbf{G} = \mathbf{G}_0 + \mathbf{G}_0\,\Delta\mathbf{H}\,\mathbf{G}$ where $\Delta\mathbf{H}$ is the change to the Hamiltonian in order to extend the system. To avoid numerical

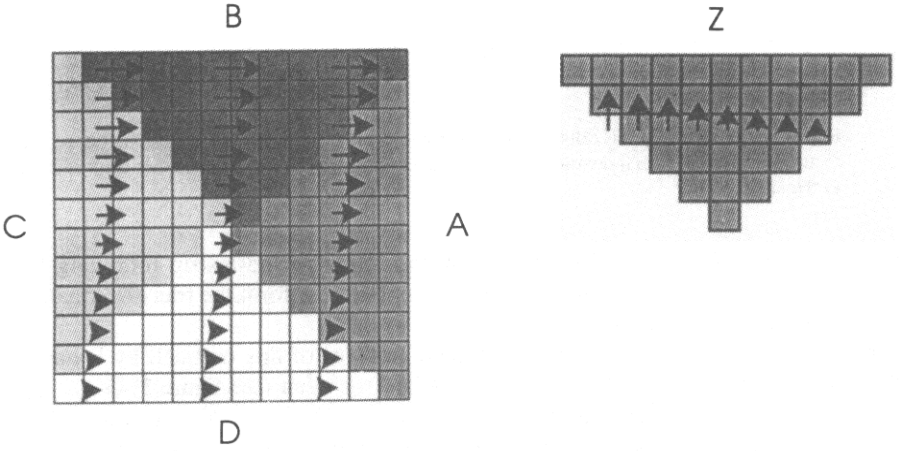

Figure 2. Example of the use of the gauge symmetry of the problem to minimize the computation needed. Rotating the triangle A gives triangle Z, in the same position as B, but in a different gauge. Applying the gauge transformation described in the text allows us to calculate the Green function for triangle B from the gauge transformation for triangle Z.

complications we work with a small imaginary part to the energy, which we exploit below to determine the group velocity.

Here we point out that by making use of the gauge symmetry of the problem we can reduce greatly the computational problem. For example we form the Green function of one square unit cell of the superlattice potential from the Green functions of the four triangles shown in figure 2, where the Green functions of the four triangles are identical up to a gauge transform. Consider finding the Green function of triangle B from triangle A. Mapping the coordinates of triangle A gives the Green function for triangle Z, with the right position, but in the wrong gauge. The general gauge transform needed is

$$\Delta \boldsymbol{A} = \left(+\alpha y + \beta_x, +\alpha x + \beta_y, 0\right). \tag{11}$$

The gauge transform is performed by multiplying the wave function at each point by $\exp(\mathrm{i}f)$ where $\nabla f = \Delta \boldsymbol{A}$. The Green function G_{IJ} between two sites I and J, in therefore transformed according to

$$\boldsymbol{A} \mapsto \boldsymbol{A}' = \boldsymbol{A} + \Delta \boldsymbol{A} \qquad G \mapsto G' = \exp[\mathrm{i}f(I)]G_{IJ}\exp[-\mathrm{i}f(J)]. \tag{12}$$

5. Application to periodic system

To evaluate the properties of the periodic system, we first use the translational symmetry in the y direction, and Fourier transform in that direction. Introducing indices X, Y for the unit cells of the full potential, and Fourier transforming with respect to Y, we have

$$H_{ik\,jk} = \sum_{Y'} H_{iY\,jY'} \exp\left[-\mathrm{i}k(Y - Y')\right] \tag{13}$$

$$G_{iY\,jY'} = \frac{1}{2\pi}\int_{-\pi}^{\pi} \mathrm{d}k\, G_{ik\,jk} \exp\left[\mathrm{i}k\left(Y - Y'\right)\right]. \tag{14}$$

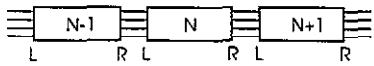

Figure 3. Labelling of the cells joined together to form an infinite one-dimensional strip. The rectangles represent the individual cells, calculated with a particular wavenumber perpendicular to the strip.

For each k we solve for the Green function of an infinite periodic strip following the method of Chase [30]. Given the Green function for a unit cell we form the transfer equation for a periodic strip in the X direction.

Let us denote the sites on the left- and right-hand surfaces of this unit cell by R and L respectively, and number the unit cells $N, N+1, N+2, \ldots$, so that (see figure 3) $\mathbf{G}_{RN-1,LN}$ is the sub-matrix of the Green function between the right side of cell $N-1$ and the left side of cell N. Applying Dyson's equation to the change from isolated cells, to an infinite strip of cells we have

$$\begin{pmatrix} \mathbf{I} & -\mathbf{G}^0_{LNLN}\mathbf{V} \\ \mathbf{0} & -\mathbf{G}^0_{RNLN}\mathbf{V} \end{pmatrix} \begin{pmatrix} \mathbf{G}_{LNM} \\ \mathbf{G}_{RN-1M} \end{pmatrix} = \begin{pmatrix} \mathbf{G}^0_{LNRN}\mathbf{V} & \mathbf{0} \\ \mathbf{G}^0_{RNRN}\mathbf{V} & -\mathbf{I} \end{pmatrix} \begin{pmatrix} \mathbf{G}_{LN+1M} \\ \mathbf{G}_{RNM} \end{pmatrix} + \begin{pmatrix} \mathbf{G}^0_{LNM} \\ \mathbf{G}^0_{RNM} \end{pmatrix} \tag{15}$$

where $\mathbf{I}$ is the identity matrix. The eigenfunctions and values of the generalized eigenvalue equation

$$\begin{pmatrix} \mathbf{I} & -\mathbf{G}^0_{LNLN}\mathbf{V} \\ \mathbf{0} & -\mathbf{G}^0_{RNLN}\mathbf{V} \end{pmatrix} \begin{pmatrix} \mathbf{G}_{LNM} \\ \mathbf{G}_{RN-1M} \end{pmatrix} = \lambda \begin{pmatrix} \mathbf{G}^0_{LNRN}\mathbf{V} & \mathbf{0} \\ \mathbf{G}^0_{RNRN}\mathbf{V} & -\mathbf{I} \end{pmatrix} \begin{pmatrix} \mathbf{G}_{LNM} \\ \mathbf{G}_{RN-1M} \end{pmatrix} \tag{16}$$

then give the eigenstates of the Schrödinger equation at the given energy.

5.1. Green function of an infinite strip

To derive the Green function in the infinite strip, it is most convenient to use Dyson's equation again, applied to $\mathbf{G}_{LNLN}$, and the sub-matrices of $\mathbf{G}$ to which it is coupled. Substituting into equation (15) the relevant choices of M, we have:

$$\begin{aligned}
\mathbf{G}_{LNLN} &= \mathbf{G}^0_{LNLN} + \mathbf{G}^0_{LNLN}\mathbf{V}\mathbf{G}_{RN-1,LN} + \mathbf{G}^0_{LNRN}\mathbf{V}^\dagger\mathbf{G}_{LN+1,LN} \\
\mathbf{G}_{RN-1,LN} &= \mathbf{G}^0_{RN-1,LN-1}\mathbf{V}\mathbf{G}_{RN-2,LN} + \mathbf{G}^0_{RN-1,RN-1}\mathbf{V}^\dagger\mathbf{G}_{LN,LN} \\
\mathbf{G}_{LN+1,LN} &= \mathbf{G}^0_{LN+1,LN+1}\mathbf{V}\mathbf{G}_{RN,LN} + \mathbf{G}^0_{LN+1,RN+1}\mathbf{V}^\dagger\mathbf{G}_{LN+2,LN} \\
\mathbf{G}_{RN,LN} &= \mathbf{G}^0_{RN,LN} + \mathbf{G}^0_{RN,LN}\mathbf{V}\mathbf{G}_{RN-1,LN} + \mathbf{G}^0_{RN,RN}\mathbf{V}^\dagger\mathbf{G}_{LN+1,LN}.
\end{aligned} \tag{17}$$

We now use the periodicity of the system to find a closed set of equations for the Green function. Let α be the (diagonal) matrix of eigenvalues for modes travelling to the left. Let $\mathbf{R}$ be a matrix with the halves of the eigenvectors corresponding to the sites on the right face of the unit cell for these modes; and let $\mathbf{L}$ be a matrix with the halves corresponding to the left face of the unit cell. Let α', $\mathbf{R}'$, $\mathbf{L}'$ be the corresponding matrices for modes travelling in the other direction. We use a sufficiently large imaginary component to the energy that

we can distinguish the eigenvalues for each direction according to whether their modulus is smaller or greater than unity [26].

Noting that $\mathbf{G}^0_{RN,RN} = \mathbf{G}^0_{RN-1,RN-1}$ etc.; writing $\mathbf{G}_{LN,LN} = \mathbf{LP}_{LN,LN}$; and using $\mathbf{G}_{RN-2,LN} = \mathbf{R}\alpha\mathbf{P}_{RN-1,LN}$ etc we obtain a closed set of equations for the Green function in the infinite system:

$$\begin{aligned}
LP_{LNLN} &= \mathbf{G}^0_{LNLN} + \mathbf{G}^0_{LNLN}\mathbf{V}RP_{RN-1,LN} + \mathbf{G}^0_{LNRN}\mathbf{V}^\dagger LP_{LN+1,LN} \\
RP_{RN-1,LN} &= \mathbf{G}^0_{RN,LN}\mathbf{V}R\alpha P_{RN-1,LN} + \mathbf{G}^0_{RN,RN}\mathbf{V}^\dagger LP_{LN,LN} \\
LP_{LN+1,LN} &= \mathbf{G}^0_{LN+1,LN+1}\mathbf{V}RP_{RN,LN} + \mathbf{G}^0_{LN+1,RN+1}\mathbf{V}^\dagger L\alpha' P_{LN+1,LN} \\
RP_{RN,LN} &= \mathbf{G}^0_{RN,LN} + \mathbf{G}^0_{RN,LN}\mathbf{V}RP_{RN-1,LN} + \mathbf{G}^0_{RN,RN}\mathbf{V}^\dagger LP_{LN+1,LN}.
\end{aligned} \tag{18}$$

Having solved these equations for the Green function on the edges of the unit cells, we can use Dyson's equation to obtain other elements of the Green function, including the diagonal elements that give the density of states.

5.2. Conductivity from transfer matrix

We now transform equation (2) into a more convenient form. Writing in full the sums over modes, we have

$$\sigma_{xx} = \frac{e^2\tau}{A}\sum_n \int_{-\pi/a_x}^{\pi/a_x} \frac{\mathrm{d}k_x}{2\pi/(N_x a_x)} \int_{-\pi/a_y}^{\pi/a_y} \frac{\mathrm{d}k_y}{2\pi/(N_y a_y)} v_x^2 \left(-\frac{\partial f}{\partial E}\right)_{E_F(k,n)} \tag{19}$$

where N_x and N_y are the number of unit cells in the x and y directions, and a_x and a_y are the dimensions of the unit cell of the full potential. Noting that $v_x = \hbar^{-1}\partial E/\partial k_x$ and changing variables from k_x, k_y to E, k_y:

$$\sigma_{xx} = \frac{e^2\tau}{4\pi^2\hbar^2}\sum_n \int \mathrm{d}E \int_{-\pi/a_y}^{\pi/a_y} \mathrm{d}k_y \left(\frac{\partial E}{\partial k_x}\right)^2 \left(\frac{\partial k_x}{\partial E}\right)\left(-\frac{\partial f}{\partial E}\right) \tag{20}$$

where the factor $\partial k_x/\partial E$ comes from the change of variables. Simplifying,

$$\sigma_{xx} = \frac{e^2\tau}{4\pi^2\hbar^2}\sum_n \int \mathrm{d}E \int_{-\pi/a_y}^{\pi/a_y} \mathrm{d}k_y \left(\frac{\partial E}{\partial k_x}\right)\left(-\frac{\partial f}{\partial E}\right). \tag{21}$$

Since we work with a small imaginary component to the energy, there is a simple way to extract $\partial k_x/\partial E$. The wavenumber k is given by $(\log\lambda)/a_x$, where λ is an eigenvalue of equation (16). Within a band $\partial k/\partial E$ is real, so the change to k caused by the imaginary part of the energy is, to first order, imaginary. We therefore have

$$\partial k/\partial E = \mathrm{Im}(k)/\mathrm{Im}(E). \tag{22}$$

With an infinitesimal imaginary part of E the expression is exact; in practice values of $\mathrm{Im}(E)/\mathrm{Re}(E)$ of the order of 10^{-4} are adequate, and numerically stable.

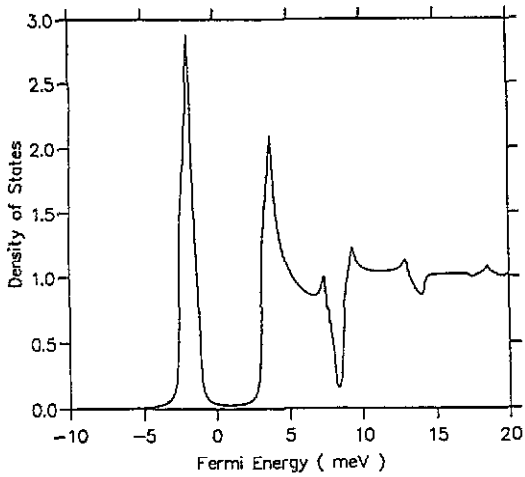

Figure 4. Density of states (relative to the density of states of a 2DEG with no applied potential) with no magnetic field present.

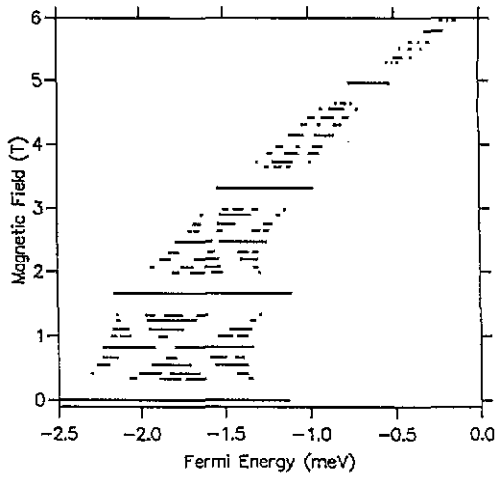

Figure 5. Spectrum of lowest tight-binding band, with magnetic fields with $p/1$, $p/2$, $p/3$, $p/4$ and $p/5$ flux quanta per unit cell, calculated with a resolution δE = 0.024 meV.

6. Density of states

We now show how the density of states can be found from the sensitivity of the eigenvalues to the energy. The details of the derivation are in the appendix. We find that the density of states is given by

$$\rho = -\frac{1}{\pi}\,\mathrm{Im}\sum\frac{\partial \log\lambda}{\partial E}. \tag{23}$$

This is a generalization to many modes, and to complex energies of the simple one-dimensional result of $\rho = \partial k/\partial E$.

The sum of derivatives of the wavenumbers can be found numerically by performing the calculation of the eigenvalues for two differing values of the imaginary component of the energy. The density of states is then given by

$$\rho = -\frac{1}{\pi\Delta\,\mathrm{Im}(E)}\,\mathrm{Re}\left(\sum\log\lambda(E+\Delta E)-\sum\log\lambda(E)\right). \tag{24}$$

Note that there is no need to identify corresponding eigenvalues at the two energies in order to perform the differentiation. Also note that $-\partial\log\lambda/\partial E$ is not necessarily positive so the individual contributions to the sum cannot be identified as the densities of states in individual modes.

7. Tight-binding limit—Hofstader's butterfly

Figure 4 shows the density of states with no magnetic field present for the potential

$$V(x,y) = \tfrac{1}{4}V_0\big[\cos(2\pi x/a)+\cos(2\pi y/a)\big] \tag{25}$$

with $V_0 = 20$ meV and $a = 50$ nm. (Note that with an infinitesimal imaginary component to the energy, the results are unchanged under the transformation $a \to a/\Lambda$, $E \to E/\Lambda^2$, $\sigma \to \sigma/\Lambda^2$, and $B \to B\Lambda^2$, where a is the lattice period, E the Fermi energy, σ the conductivity, B the magnetic field, and Λ a scaling factor.)

As an example, we have examined how the tight-binding like band at low energy evolves with magnetic field. With a magnetic field and a periodic potential present, we expect a recursively split spectrum. Figure 5 shows the spectrum for fields with up to five flux quanta per unit cell. With p/q flux quanta per unit cell the band is split into q subbands. The recursively split spectrum of Hofstader's butterfly [4] with the band split into q subbands when there are p/q flux quanta per unit cell is clearly seen.

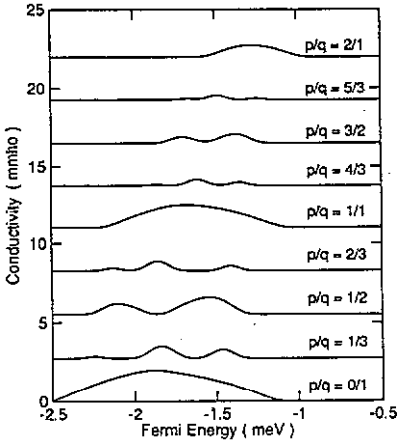

Figure 6. Band conductivity in lowest tight-binding band for fields with different numbers p/q of flux quanta per unit cell.

Using our method we can readily evaluate the band conductivity for this case. Figure 6 shows some representative results calculated with $\tau = 38$ ps and a temperature of 0.3 K. The results show the expected suppression of the band conductivity for larger values of q. The results show that the mean free path of an electron in this limit, assuming the fixed relaxation time, is of the order of 2000 nm. In practice electron interaction effects are likely to be important in this single-band limit, where there is of the order of one electron per unit cell. A rough estimate of the relevant energy scale is the interaction energy between two electrons separated by a lattice constant, $e^2/4\pi\epsilon a = 2$ meV, which is comparable to the bandwidth. At higher electron densities screening, and the larger bandwidths, will reduce the importance of electron interactions, and we address this limit in a future paper.

8. Conclusions

We have shown how the recursive Green-function method can be used to calculate the band conductivity and density of states of lateral-surface superlattices in the presence of magnetic fields. By including an imaginary component to the energy, we can deduce the group velocity of the states at a given energy. By calculating the sensitivity of the wavenumbers of the states to the imaginary part of the energy, or by directly calculating the diagonal elements of the Green function we can calculate the density of states.

As a simple example we have shown results for a superlattice in the tight-binding limit, and shown the energy scale on which Hofstader's butterfly exists. In practice the recursive spectrum is likely to be unobservable in this limit, because of the effects of disorder [31] and the Coulomb blockade [11, 12, 14, 32]. Results for regimes where commensurability effects are likely to be more easily observed are in preparation.

Appendix

We now show in detail how the density of states can be found from the sensitivity of the eigenvalues to the energy. To show the relationship we use the full Hamiltonian for the strip, rather than using the Green function on the surface of the unit cells, and the components of the Hamiltonian between cells as above.

The Green function of the system satisfies

$$\begin{pmatrix} \mathbf{V}^\dagger & \mathbf{0} \\ \mathbf{0} & \mathbf{I} \end{pmatrix} \begin{pmatrix} \mathbf{G}_{N+1\,M} \\ \mathbf{G}_{N\,M} \end{pmatrix} = \begin{pmatrix} (\mathbf{E}-\mathbf{H}) & -\mathbf{V} \\ \mathbf{I} & \mathbf{0} \end{pmatrix} \begin{pmatrix} \mathbf{G}_{N\,M} \\ \mathbf{G}_{N-1\,M} \end{pmatrix} + \mathbf{I}\delta_{\mathbf{NM}} \tag{A1}$$

where $\mathbf{H}$ is the Hamiltonian between sites in one unit cell, $\mathbf{V}$ is the Hamiltonian between sites in unit cell N and cell $N-1$, and $\mathbf{V}^\dagger$ is the Hamiltonian between sites in cell $N-1$ and cell N. We first derive an explicit formula for the Green function in terms of the eigenstates of the homogeneous equation

$$\alpha \begin{pmatrix} \mathbf{V}^\dagger & \mathbf{0} \\ \mathbf{0} & \mathbf{I} \end{pmatrix} \begin{pmatrix} \alpha\chi \\ \chi \end{pmatrix} = \begin{pmatrix} E-H & -\mathbf{V} \\ \mathbf{I} & \mathbf{0} \end{pmatrix} \begin{pmatrix} \alpha\chi \\ \chi \end{pmatrix} \tag{A2}$$

where by construction the eigenvectors have the form indicated. We then show how the Green function can be found in terms of the derivatives of the eigenvalues with respect to the energy.

Because the term $\mathbf{V}$ only couples sites on the surface of the unit cell, $\mathbf{V}$ is in general singular. The eigenvalues of equation (A2), however, are the same as those of equation (16), except for the inclusion of modes with $\mathbf{V}\chi = \mathbf{0}$, which do not contribute to the surface Green function. In the following section we consider only the subspace of states for which $\mathbf{V}\chi$ is not singular. The existence of states for which $\mathbf{V}\chi = \mathbf{0}$ is an artifact of working on a discrete lattice, where only a finite number of modes exist on the surface. We therefore expect the states that we are excluding to be unimportant for energies where the discrete lattice is a good approximation to the continuum. Comparison of the results of the formula we will describe, and the density of states calculated directly from the Green function, confirm this.

Let $\mathbf{u}$ be the matrix whose columns are the upper halves, χ, of the eigenvectors propagating to the right, and let λ be the corresponding diagonal matrix of eigenvalues. Let $\mathbf{w}$ and γ be the corresponding matrices for modes travelling to the left. Writing the components of the Green function in terms of the eigenvectors of (A2) so that $\mathbf{G}_{N+X\,N} = \mathbf{u}\lambda^X\mathbf{P}_+$, $\mathbf{G}_{N-X\,N} = \mathbf{w}\gamma^{-X}\mathbf{P}_-$ and $\mathbf{G}_{N\,N} = \mathbf{u}\mathbf{P}_0$, the equation for the Green function gives

$$\mathbf{V}^\dagger\mathbf{u}\lambda\mathbf{P}_+ = (\mathbf{E}-\mathbf{H})\mathbf{u}\mathbf{P}_0 - \mathbf{V}\mathbf{w}\gamma^{-1}\mathbf{P}_- - \mathbf{I} \tag{A3}$$

$$\mathbf{V}^\dagger\mathbf{u}\lambda^2\mathbf{P}_+ = (\mathbf{E}-\mathbf{H})\mathbf{u}\lambda\mathbf{P}_+ - \mathbf{V}\mathbf{u}\mathbf{P}_0 \tag{A4}$$

$$\mathbf{V}^\dagger\mathbf{u}\mathbf{P}_0 = (\mathbf{E}-\mathbf{H})\mathbf{w}\gamma^{-1}\mathbf{P}_- - \mathbf{V}\mathbf{w}\gamma^{-2}\mathbf{P}_-. \tag{A5}$$

The matrices $\mathbf{u}$ and $\mathbf{w}$ fulfil the equations

$$\mathbf{V}^\dagger\mathbf{u}\lambda = (\mathbf{E}-\mathbf{H})\mathbf{u} - \mathbf{V}\mathbf{u}\lambda^{-1} \tag{A6}$$

and

$$\mathbf{V}^\dagger\mathbf{w}\gamma = (\mathbf{E}-\mathbf{H})\mathbf{w} - \mathbf{V}\mathbf{w}\gamma^{-1}. \tag{A7}$$

Using equations (A5) and (A6) and equations (A4) and (A7) we find that

$$\mathbf{P}_+ = \mathbf{P}_0 = \mathbf{u}^{-1}\mathbf{w}\mathbf{P}_-. \tag{A8}$$

Substituting into (A3), and rearranging using (A6)

$$\mathbf{P}_0 = \left[\mathbf{V}^{\dagger}(\mathbf{w}\gamma\mathbf{w}^{-1}\mathbf{u} - \mathbf{u}\lambda)\right]^{-1} \tag{A9}$$

so that

$$\mathbf{G}_{nn} = \mathbf{u}\mathbf{P}_0 = 1/\mathbf{V}^{\dagger}(\mathbf{w}\gamma\mathbf{w}^{-1} - \mathbf{u}\lambda\mathbf{u}^{-1}). \tag{A10}$$

Writing (A2) in terms of the matrices $\mathbf{u}$ and $\mathbf{w}$,

$$\begin{pmatrix} \mathbf{u} & \mathbf{w} \\ \mathbf{u}\lambda^{-1} & \mathbf{w}\gamma^{-1} \end{pmatrix}\begin{pmatrix} \lambda & 0 \\ 0 & \gamma \end{pmatrix} = \begin{pmatrix} \mathbf{V}^{\dagger -1}(\mathbf{E}-\mathbf{H}) & -\mathbf{V}^{\dagger -1} \\ \mathbf{I} & 0 \end{pmatrix}\begin{pmatrix} \mathbf{u} & \mathbf{w} \\ \mathbf{u}\lambda^{-1} & \mathbf{w}\gamma^{-1} \end{pmatrix} \tag{A11}$$

Equation (A11) has the form $\phi_n\lambda_n = T\phi_n$. considering a perturbation ΔT, and keeping the terms linear in the perturbation, we have

$$\phi_n\Delta\lambda_n + \phi\Delta\lambda_n = T\Delta\phi_n + \Delta T\phi_n. \tag{A12}$$

Let ϕ_n' be the left-handed eigenvectors of T, such that $\phi_m'\phi_n = \delta_{nm}$. Multiplying on the left by ϕ_n' gives

$$\Delta\lambda_n = \phi_n^{-1}\Delta T\phi_n. \tag{A13}$$

The matrix of left-handed eigenvectors, orthogonal to the eigenvectors of equation (A11) is

$$\begin{pmatrix} \mathbf{u} & \mathbf{w} \\ \mathbf{u}\lambda^{-1} & \mathbf{w}\gamma^{-1} \end{pmatrix}^{-1} = \begin{pmatrix} (\mathbf{u} - \mathbf{w}\gamma\mathbf{w}^{-1}\mathbf{u}\lambda^{-1}) \in v & -(\mathbf{w}\gamma^{-1}\mathbf{w}^{-1}\mathbf{u} - \mathbf{u}\lambda^{-1})^{-1} \\ (\mathbf{w} - \mathbf{u}\lambda\mathbf{u}^{-1}\mathbf{w}\gamma^{-1})^{-1} & -(\mathbf{u}\lambda^{-1}\mathbf{u}^{-1}\mathbf{w} - \mathbf{w}\gamma^{-1})^{-1} \end{pmatrix}. \tag{A14}$$

Taking a perturbation ΔE in equation (A11) and multiplying the right-hand side of the equation by the inverse matrix, equation (A14), gives

$$\begin{aligned} &\begin{pmatrix} (\mathbf{u} - \mathbf{w}\gamma\mathbf{w}^{-1}\mathbf{u}\lambda^{-1})^{-1} & -(\mathbf{w}\gamma^{-1}\mathbf{w}^{-1}\mathbf{u} - \mathbf{u}\lambda^{-1})^{-1} \\ (\mathbf{w} - \mathbf{u}\lambda\mathbf{u}^{-1}\mathbf{w}\gamma^{-1})^{-1} & -(\mathbf{u}\lambda^{-1}\mathbf{u}^{-1}\mathbf{w} - \mathbf{w}\gamma^{-1})^{-1} \end{pmatrix} \\ &\quad = \begin{pmatrix} \mathbf{V}^{\dagger -1} & 0 \\ 0 & 0 \end{pmatrix}\begin{pmatrix} \mathbf{u} & \mathbf{w} \\ \lambda^{-1}\mathbf{u} & \gamma^{-1}\mathbf{w} \end{pmatrix}\Delta E \\ &\quad = \begin{pmatrix} (\mathbf{u} - \mathbf{w}\gamma\mathbf{w}^{-1}\mathbf{u}\lambda^{-1})^{-1}\mathbf{V}^{\dagger -1}\mathbf{u} & (\mathbf{u} - \mathbf{w}\gamma\mathbf{w}^{-1}\mathbf{u}\lambda^{-1})^{-1}\mathbf{V}^{\dagger -1}\mathbf{w} \\ (\mathbf{w} - \mathbf{u}\lambda\mathbf{u}^{-1}\mathbf{w}\gamma^{-1})^{-1}\mathbf{V}^{\dagger -1}\mathbf{u} & (\mathbf{w} - \mathbf{u}\lambda\mathbf{u}^{-1}\mathbf{w}\gamma^{-1}) \in v\mathbf{V}^{\dagger -1}\mathbf{w} \end{pmatrix}\Delta E \end{aligned} \tag{A15}$$

The diagonal elements of (A15) give the values of $\partial\lambda/\partial E$ and $\partial\gamma/\partial E$. Let $\mathbf{Q}$ be the upper left hand sub-matrix of equation (A15),

$$\mathbf{Q} = (\mathbf{u} - \mathbf{w}\gamma\mathbf{w}^{-1}\mathbf{u}\lambda)^{-1}\mathbf{V}^{\dagger -1}\mathbf{u}. \tag{A16}$$

The diagonal elements of $\lambda^{-1}\mathbf{Q}$ are then $\partial\log(\lambda)/\partial E$. Simplifying, we find that

$$\mathbf{u}\lambda^{-1}\mathbf{Q}\mathbf{u}^{-1} = 1/\mathbf{V}^{\dagger}(\mathbf{u}\lambda\mathbf{u}^{-1} - \mathbf{w}\gamma\mathbf{w}^{-1}) = \mathbf{G}_{NN}. \tag{A17}$$

Taking the trace of equation (A17) and noting that $\mathrm{Tr}\,ABA^{-1} = \mathrm{Tr}\,A$ we have

$$\mathrm{Tr}\,\mathbf{G}_{NN} = \sum \frac{\partial\log\lambda}{\partial E} \tag{A18}$$

and so the density of states is given by

$$\rho = -\frac{1}{\pi}\,\mathrm{Im}\sum\frac{\partial\log\lambda}{\partial E}. \tag{A19}$$

References

[1] Claro F and Wannier G H 1970 *Phys. Rev.* B **19** 6068
[2] Thouless D J, Kohmoto M, Nightingale M P and den Nijs M 1982 *Phys. Rev. Lett.* **49** 405
[3] Wilkinson M 1987 *J. Phys. A: Math. Gen.* **20** 1761
[4] Hofstader D R 1976 *Phys. Rev.* B **14** 2239
[5] Kirczenow G 1992 *Surf. Sci.* **263** 330
[6] Weiss D, von Klitzing K, Ploog K and Weinmann G 1990 *Surf. Sci.* **229** 88
[7] Weiss D, Grambow P, von Klitzing K, Menschig A and Weimann G 1991 *Appl. Phys. Lett.* **58** 2960
[8] Liu C T, Tsui D C, Shayegan M, Ismail K, Antoniadis D A and Smith H I 1991 *Appl. Phys. Lett.* **58** 25
[9] Fang H and Stiles P J 1990 *Phys. Rev.* B **41** 10171
[10] Ensslin K and Petroff P M 1990 *Phys. Rev.* B **41** 12307
[11] Scott-Thomas J H F, Field S B, Kastner M A, Smith H I and Antoniadia D A 1989 *Phys. Rev. Lett.* **62** 583
[12] van Houten H and Beenakker C W J 1989 *Phys. Rev. Lett.* **63** 1893
[13] Beenakker C W J 1991 *Phys. Rev.* B **44** 1646
[14] McEuen P L, Foxman E B, Meirav U, Kastner M A, Meir Y and Wingreen N S 1991 *Phys. Rev. Lett.* **66** 1926
[15] Tsui D C, Störmer H L and Grossard A C 1982 *Phys. Rev. Lett.* **48** 1559
[16] Laughlin R B 1983 *Phys. Rev. Lett.* **50** 1395
[17] Zhang C and Gerhardts R R 1990 *Phys. Rev.* B **41** 12850
[18] Vasilopoulos P and Peeters F M 1989 *Phys. Rev. Lett.* **63** 2120
[19] Wulf U, Gudmundsson V and Gerhardts R R 1988 *Phys. Rev.* B **38** 4218
[20] Gudmundsson V and Gerhardts R R 1987 *Phys. Rev.* B **35** 8005
[21] Degani M and Leburton J P 1991 *Phys. Rev.* B **44** 10901
[22] von Klitzing K, Dorda G and Pepper M 1980 *Phys. Rev. Lett.* **45** 494
[23] Halperin B I 1982 *Phys. Rev.* B **25** 1285
[24] Büttiker M 1988 *Phys. Rev.* B **38** 9375
[25] Pendry J B, Prêtre A, Rous P J and Martín-Moreno L 1991 *Surf. Sci.* **244** 160
[26] MacKinnon A 1985 *Z. Phys.* B **59** 385
[27] MacKinnon A 1980 *J. Phys. C: Solid State Phys.* **12** L1031
[28] Thouless D J and Kirkpatrick S 1981 *J. Phys. C: Solid State Phys.* **14** 235
[29] Sols F, Macucci M, Ravaioli U and Hess K 1989 *J. Appl. Phys.* **66** 3892
[30] Chase K S 1986 *PhD Thesis* Imperial College
[31] Nixon J A and Davies J H 1990 *Phys. Rev.* B **41** 7929
[32] Beenakker C W J and van Houten H 1989 *Phys. Rev. Lett.* **63** 1857